Electron Spin Resonance Study of the pH-Induced Transformation of Micelles to Vesicles in an Aqueous Oleic Acid/Oleate System

Hiroshi Fukuda,[†] Ayako Goto,*[,†] Hisashi Yoshioka,[‡] Rensuke Goto,[‡] Kenichi Morigaki,[§] and Peter Walde[§]

School of Informatics and Graduate School of Nutritional and Environmental Sciences, University of Shizuoka, Yada 52-1, Shizuoka-shi, 422-8526 Japan, and Institut für Polymere, ETH-Zürich, Universitätstrasse 6, CH-8092 Zürich, Switzerland

Received January 8, 2001. In Final Form: April 25, 2001

ESR (electron spin resonance) spectra of a fatty acid spin probe (16-doxylstearic acid, 16-DS) incorporated into an aqueous surfactant system composed of oleic acid and oleate molecules were measured between 10 and 50 °C up to a total oleic acid + oleate concentration of 50 mM. Depending on the total concentration and the pH, different types of oleic acid/oleate aggregates formed. At the two ends of the pH range investigated (above pH 10.4 and below pH 6.4), the ESR spectra of 16-DS were highly symmetric, enabling calculation of the microviscosities in the surfactant aggregates to be 4 cP and 6 cP, respectively. In the high pH range, the observed aggregates are micelles. On the other hand, in the low pH range the microviscosity was considerably lower than that of neat oleic acid (measured to be 11 cP), indicating that the obtained emulsion system was not composed of pure oleic acid droplets. We postulate that the surfactant molecules at low pH form condensed aggregates of lamellar bilayers. Asymmetric high-field ESR lines were obtained at intermediate pH between pH 6.4 and pH 10.4. This indicates that the probe molecules were present in two physically different aggregation states. We assigned the two aggregation states to be vesicles and nonlamellar aggregates (most likely nonspherical micelles), based on the observation made by microscopy and light scattering techniques. The analysis of the ESR lines by spectral simulation using a modified Bloch equation supports the coexistence of vesicles and nonlamellar aggregates through the entire intermediate pH range; the relative amount of the two aggregation forms depends critically on pH, temperature, and concentration. Furthermore, the spectral simulation indicated that particularly stable oleic acid/oleate vesicles are formed around pH 8.5, where the protonated and ionized species exist in a stoichiometric ratio.

Introduction

The vesicle formation from surfactant molecules with a single hydrocarbon chain has attracted considerable attention in recent years.[1−16] Because single-chain surfactants very often tend to form micelles, the bilayer formation is usually induced by the modification of the experimental conditions such as surfactant composition, ionic strength, or pH. The mechanistic understanding of the micelle−vesicle transition bears profound significance both in the biological sciences and technological applications, and extensive studies have been devoted to it. For example, Söderman et al.[17] studied the micelle−vesicle transition in the case of two oppositely charged surfactants, a so-called catanionic system.[4−7,9,12−15] On the basis of light scattering, NMR, and fluorescence quenching experiments, a limited growth of the micelles with changes in composition could be observed, before vesicles abruptly started to be formed at a characteristic mixing ratio of the two surfactants. As the composition moved further into the vesicle region, the quantity of micelles decreased gradually. The transition from micelles to vesicles in this particular system seems to be a continuous process.[17]

With respect to the micelle−vesicle transformation, the soap/fatty acid/water system is particularly interesting because only one type of amphiphile is involved.[1,3,8,18−22]

* Corresponding author. Tel/Fax: +81-54-264-5238. E-mail: gotoa@momo1.u-shizuoka-ken.ac.jp.

† School of Informatics, University of Shizuoka.

‡ Graduate School of Nutritional and Environmental Sciences, University of Shizuoka.

§ Institut für Polymere, ETH-Zürich.

(1) Gebicki, J. M.; Hicks, M. *Nature* **1973**, *243*, 232−234.

(2) Hargreaves, W. R.; Deamer, D. W. *Biochemistry* **1978**, *17*, 3759−3768.

(3) Bittman, R.; Blau, L. *Biochim. Biophys. Acta* **1986**, *863*, 115−120.

(4) Kaler, E. W.; Murthy, A. K.; Rodriguez, B. E.; Zasadzinski, J. A. N. *Science* **1989**, *245*, 1371−1374.

(5) Fukuda, H.; Kawata, K.; Okuda, H.; Regen, S. L. *J. Am. Chem. Soc.* **1990**, *112*, 1635−1637.

(6) Kaler, E. W.; Herrington, K. L.; Murthy, A. K.; Zasadzinski, J. A. N. *J. Phys. Chem. B* **1992**, *96*, 6698−6707.

(7) Ambühl, M.; Bangerter, F.; Luisi, P. L.; Skrabal, P.; Watzke, H. J. *Langmuir* **1993**, *9*, 36−38.

(8) Walde, P.; Wick, R.; Fresta, M.; Mangone, A.; Luisi, P. L. *J. Am. Chem. Soc.* **1994**, *116*, 11649−11654.

(9) Yatcilla, M. T.; Herrington, K. L.; Brasher, L. L.; Kaler, E. W.; Chriuvolu, S.; Zasadzinski, J. A. *J. Phys. Chem. B* **1996**, *100*, 5874−5879.

(10) Berström, M.; Eriksson, J. C. *Langmuir* **1996**, *12*, 624−635.

(11) Walde, P.; Wessicken, M.; Rädler, U.; Berclaz, N.; Conde-Frieboes, K.; Luisi, P. L. *J. Phys. Chem. B* **1997**, *101*, 7390−7397.

(12) Marques, E. F.; Regev, O.; Khan, A.; da Graça Miguel, M.; Lindman, B. *J. Phys. Chem. B* **1998**, *102*, 6746−6578.

(13) Salkar, R. A.; Mukesh, D.; Samant, S. D.; Manohar, C. *Langmuir*, **1998**, *14*, 3778−3782.

(14) Hoffmann, H.; Gräbner, D.; Hornfeck, U.; Platz, G. *J. Phys. Chem. B* **1999**, *103*, 611−614.

(15) Villeneuve, M.; Kaneshina, S.; Imae, T.; Areatono, M. *Langmuir* **1999**, *15*, 2029−2036.

(16) Buwalda, R. T.; Stuart, M. C. A.; Engberts, J. B. F. N. *Langmuir* **2000**, *16*, 6780−7686.

(17) Söderman, O.; Herrington, K. L.; Kaler, E. W.; Miller, D. D. *Langmuir* **1997**, *13*, 5531−5538.

(18) Gebicki, J. M.; Hicks, M. *Chem. Phys. Lipids* **1976**, *16*, 142−160.

(19) Haines, T. H. *Proc. Natl. Acad. Sci. U.S.A.* **1983**, *80*, 160−164.

(20) Cistola, D. P.; Atkinson, D.; Hamilton, J. A.; Small, D. M. *Biochemistry* **1986**, *25*, 2804−2812.

10.1021/la0100338 CCC: $20.00
Published on Web 06/01/2001

Chart 1. Chemical Structures of Oleic Acid and 16-Doxylstearic Acid (16-DS)

Oleic acid

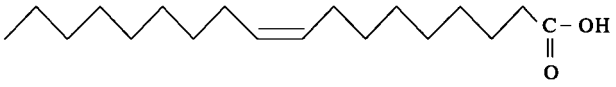

16-Doxyl-stearic acid

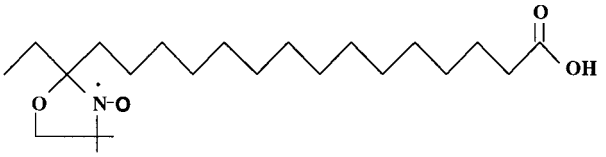

Under alkaline pH conditions, long-chain fatty acid salts (soaps) are known to form micelles above the Kraft temperature and above the critical concentration for micelle formation (cmc).[23,24] With decreasing pH, vesicles start to form in the micellar solution.[1−3,8,18−22,24−26] Cryo-transmission electron microscopy showed that the vesicles which are formed in partly protonated aqueous oleate samples are often unilamellar.[27]

In previous studies, we have observed that the size distributions of the vesicles are strongly influenced by various external factors. For example, the formation of unilamellar giant vesicles was promoted by dilution of the vesicle suspensions.[26] Furthermore, we reported recently that the size distribution of newly formed vesicles was affected by the vesicles that had been already in the aqueous phase.[28]

To obtain insight into the kinetic and equilibrium aspects of the oleic acid/oleate/water system, we conducted a systematic study of the microviscosity of the surfactant aggregates using electron spin resonance (ESR) spectroscopy. A fatty acid derivative (16-doxylstearic acid, 16-DS, see Chart 1) was used as the spin probe, and ESR spectra were measured as a function of pH, temperature, and the surfactant concentration. A detailed analysis of the high-field ESR lines was carried out with the aid of a computer simulation based on a modified Bloch equation.

The ESR measurements and the simulation indicated the coexistence of nonlamellar aggregates and bilayers in the pH region, in which vesicles had been previously regarded to be the only aggregation form. The presence of nonlamellar aggregates, that could be a type of micelles, may reflect the dynamic nature of the single-chain surfactant aggregates in water.

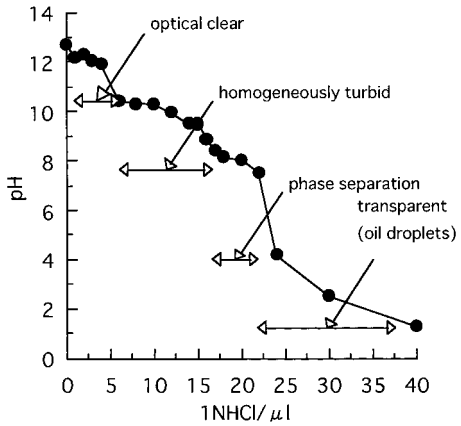

Figure 1. Equilibrium titration curve for 1 mL of 26.7 mM sodium oleate to which 1 M HCl was added at 25 °C.

Materials and Methods

Sodium oleate was purchased from Sigma (USA). 16-Doxylstearic acid (16-DS), which is stearic acid spin-labeled at the 16th carbon, was obtained from Aldrich (USA) and was used as a spin probe. Sodium oleate solutions at a concentration of 25 mM were prepared by dissolving sodium oleate in pure water. 16-DS was dissolved in acetone, and an aliquot of 50 μL was put into a test tube. After complete evaporation of acetone, 1.5 mL of a micellar solution of sodium oleate was added and the spin probe was dispersed by bath sonication for 15 s (molar ratio [16-DS]/[sodium oleate] = 1:200). The pH was adjusted to the desired value by the addition of small amounts of 1 M HCl or 1 M NaOH. The samples were then equilibrated for 12−15 h at 25 °C before use.

Egg lecithin (a mixture of egg phosphatidylcholines, egg PC, Coatsome NC-10S) was purchased from Nippon Oils & Fats Co. Ltd. Egg PC vesicle suspensions were prepared by first dissolving egg PC in 3 mL of methanol in a test tube. Methanol was then removed under reduced pressure with a rotatory evaporator. The resulting lipid film was dispersed under vortexing in an appropriate amount of water to yield an egg PC concentration of 5 mM. Sodium dodecyl sulfate (SDS) was obtained from Wako Pure Chemicals Co., Tokyo.

ESR spectra were recorded on a JEOL JESRE3X spectrometer, equipped with a variable temperature accessory between 10 and 50 °C, using a flat quartz cell. The ESR spectra of 16-DS were measured in the presence of various amounts of sodium oleate + oleic acid (0−50 mM) at a temperature between 10 and 50 °C. Mn^{2+} in MgO was used as an external reference in order to get precise peak positions.

The mean size and the size distribution of the oleic acid/oleate aggregates were measured by an electrophoretic light scattering photometer (ELS800 from Otsuka Electronics Co., Japan).

Results

Oleate/Oleic Acid Titration Curve. Figure 1 shows the equilibrium titration curve for a dilute sodium oleate/oleic acid/water system at 25 °C. This curve was obtained by first dissolving sodium oleate at a concentration of 26.7 mM in pure water and adjusting the pH to 12.5 with a small amount of 1 M NaOH. Upon addition of HCl to this alkaline solution, the pH dropped, resulting in a protonation of the carboxylate group. The solution remained transparent down to a pH of 10.4. In the range 10.4 > pH > 8.0, the system was homogeneously turbid, at 8.0 > pH > 4.2 phase separation occurred, and at pH < 3 oil droplets of oleic acid were clearly separated from the aqueous phase.

ESR Spectra of 16-DS Incorporated in the Oleic Acid/Oleate System. *(a) Initial Observations in the Entire pH Range.* Figure 2 shows the ESR spectra of 16-DS in the presence of 25 mM sodium oleate/oleic acid at pH 12.1, pH 8.7, and pH 6.4 in the absence of any buffers.[29] If one makes a qualitative comparison of the three spectra, the

(21) Cistola, D. P.; Hamilton, J. A.; Jackson, D.; Small, D. M. *Biochemistry* **1988**, *27*, 1881−1888. Please note that the apparent pK_a of oleic acid in the oleic acid/oleate aggregates is higher (ca. 8.5) than one expects from the pK_a of a water soluble carboxylic acid (ca. 4.7). This can be explained as a consequence of the accumulation of H^+ on the surface of the aggregates which leads to a decrease of the local pH. The intrinsic pK_a of oleic acid in the aggregates is probably not much different from 4.7.

(22) Morigaki, K.; Dallavalle, S.; Walde, P.; Colonna, S.; Luisi, P. L. *J. Am. Chem. Soc.* **1997**, *119*, 292−301.

(23) Reiss-Husson, F.; Luzzati, V. *J. Phys. Chem.* **1964**, *68*, 3504−3511.

(24) Small, D. M. *The Physical Chemistry of Lipids*; Handbook of Lipid Research 4; Plenum Press: New York, 1986.

(25) Wick, R.; Walde, P.; Luisi, P. L. *J. Am. Chem. Soc.* **1995**, *117*, 1435−1436.

(26) Goto, A.; Suzuki, A.; Yoshioka, H.; Goto, R.; Imae, T.; Yamazaki, K.; Walde, P. In *Giant Vesicles*; Luisi, P. L., Walde, P., Eds.; Perspectives in Supramolecular Chemistry, Vol. 6; John Wiley & Sons, Ltd.: Chichester, 2000; Chapter 19.

(27) Edwards, K.; Silvander, M.; Karlsson, G. *Langmuir* **1995**, *11*, 2429−2434.

(28) Blöchliger, E.; Blocher, M.; Walde, P.; Luisi, P. L. *J. Phys. Chem. B* **1998**, *102*, 10383−10390.

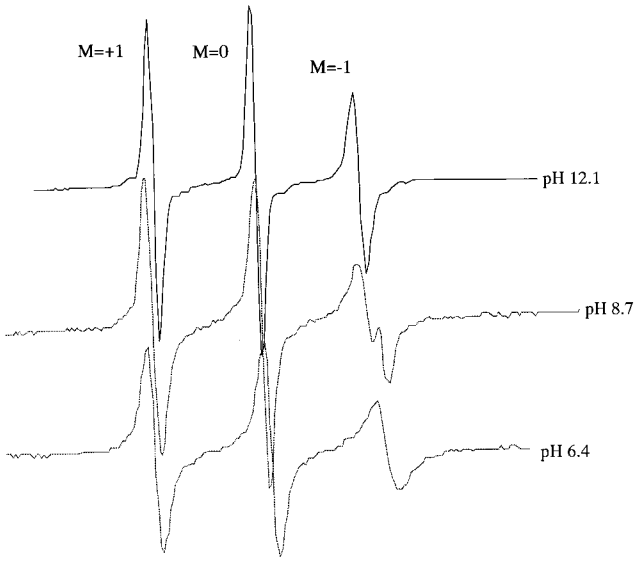

Figure 2. ESR spectra of 16-DS in 25 mM sodium oleate/oleic acid measured at pH 12.1, 8.7, and 6.4.

following is obvious: (i) in all three cases, the lines at $M = +1$ and at $M = 0$ are symmetric; (ii) whereas the high-field line at $M = -1$ in the high and low pH cases (pH 12.1 and pH 6.4) is highly symmetric, it is asymmetric at pH 8.7 as a result of the overlapping of at least two different lines.

The rotation of the spin probe is reflected in the height and the width of the ESR lines as shown in eq 1 (see below): the higher the peak-to-peak height and the smaller the peak-to-peak width, the faster the rotation of the spin probe. In Figure 3A,B, the peak-to-peak height ($I_{M=+1}$) and the peak-to-peak width ($\Delta H_{M=+1}$) of the constantly symmetric $M = +1$ line are shown as a function of pH. Both remain constant above pH 10 but shift gradually as the pH is decreased below pH 10. Figure 3A,B indicates that the rotation of the probe above pH 10 is faster than that below pH 7, suggesting that the micelles are "softer" than the aggregation form at low pH.

The value of the hyperfine coupling constant (a_N) of 16-DS, which corresponds to the distance between the $M = +1$ and the $M = 0$ line, is plotted against pH in Figure 3C. Above pH 10 and below pH 7.5, the a_N value is nearly constant (~15.4 and 14.5 G, respectively). Between pH 10 and pH 7.5, a_N decreases continuously with decreasing pH. Although it is known that a_N is small in nonpolar solvents and becomes larger in polar solvents,[30] a_N does not simply depend on the dielectric constant of the medium. In the case of solvents possessing a hydroxyl group, for example, the hydroxyl group stabilizes the polar structure of the N−O group of the spin probe through hydrogen bonding, which leads to an increase in the density of the unpaired electron, resulting in an increase of a_N. As shown in Figure 3C, a_N in the oleate micelles at high pH is higher than in the aggregates and bilayers at low pH. This is most likely due to a penetration of water molecules into the micelles.[31]

Figure 3A−C indicates that the ESR signals in different pH regions reflect the changes of microenvironment in which the spin probe molecules are located.

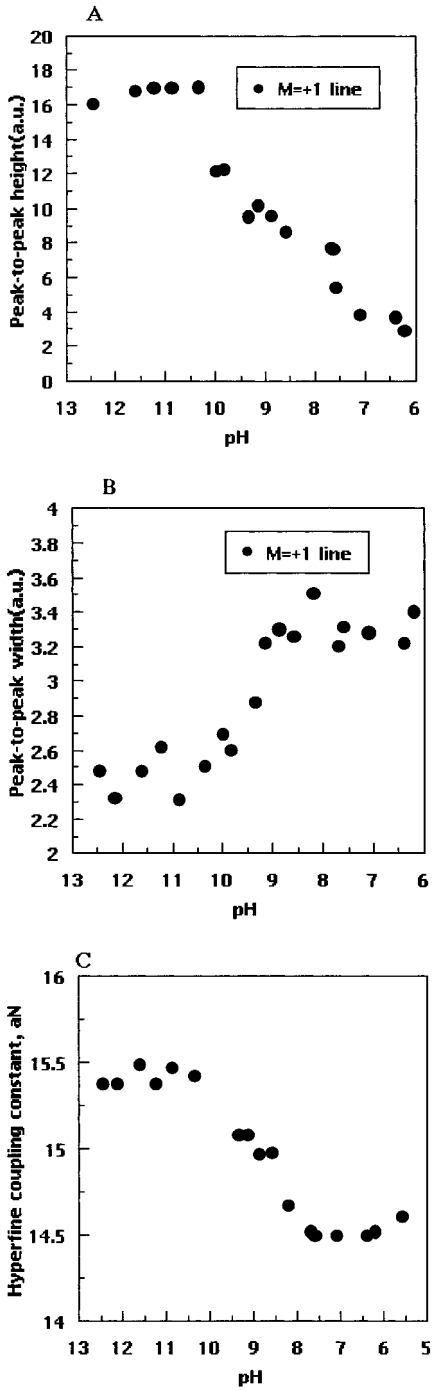

Figure 3. Peak-to-peak height (A), peak-to-peak width (B), and hyperfine coupling constants, a_N (C), of the ESR spectrum of 16-DS in 25 mM sodium oleate/oleic acid as a function of pH.

(b) The Case of High and Low pH (pH ≥ 10.4 and pH ≤ 6.4). At pH 12.1, where sodium oleate is known to form micelles above the cmc,[23,27,32−37] the ESR spectrum was measured as a function of sodium oleate concentration up

(29) The presence of buffer ions, in particular at high concentrations, may significantly influence the aggregation behavior. Bicine buffer (*N*,*N*-bis(2-hydroxyethyl)glycine) at a concentration of 200 mM and at a pH ≥ 11 induced gelation of the oleate solution, clearly indicating the presence of elongated structures.

(30) Seelig, J. In *Spin Labeling. Theory and Applications*; Berliner, L. J., Ed.; Academic Press: New York, 1976; Chapter 10.

(31) Yoshioka, H. *J. Am. Chem. Soc.* **1979**, *101*, 28−32.

(32) Stenius, P.; Palonen, H.; Ström, G.; Oedberg, L. In *Surfactants in Solution*; Mittal, K. L., Lindman, B., Eds.; Plenum Press: New York, 1984; Vol. 1, pp 153−174.

(33) Terui, G. *Phys. Lett. A* **1987**, *120*, 89−94.

(34) Mahieu, N.; Canet, D.; Cases, J. M.; Boubel, J. C. *J. Phys. Chem.* **1991**, *95*, 1844−1846.

(35) Sigehuzi, T.; Kadonaga, M.; Yamamoto, J.; Okano, K. *J. Phys. Soc. Jpn.* **1992**, *61*, 4033−4040.

(36) Lin, Z.; Eads, C. D. *Langmuir* **1997**, *13*, 2647−2654.

(37) Kaibara, K.; Iwata, E.; Eguchi, Y.; Suzuki, M.; Maeda, H. *Colloid Polym. Sci.* **1997**, *275*, 77−783.

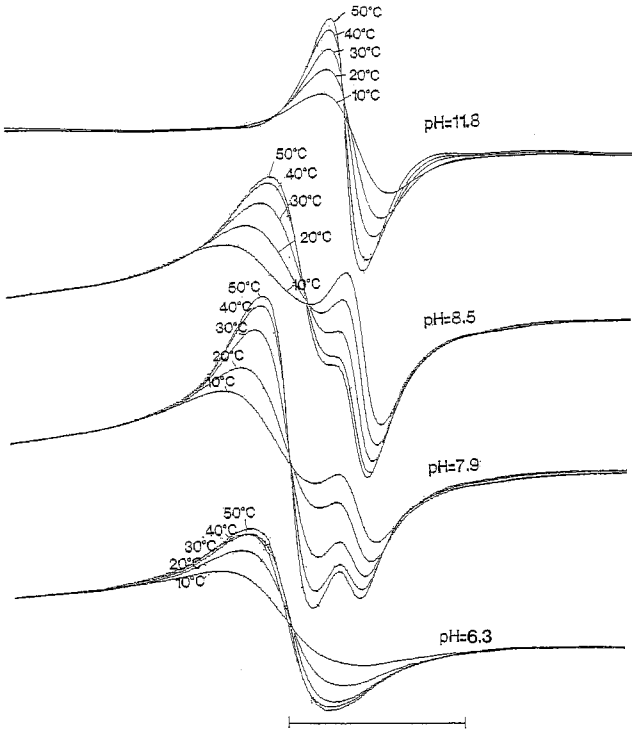

Figure 4. Effect of temperature on the ESR spectrum of 16-DS in 25 mM sodium oleate/oleic acid at different pH values. The bar corresponds to 0.5 mT.

to 50 mM, and it was found that the shapes of all three lines at $M = +1$, at $M = 0$, and at $M = -1$ are symmetric at all concentrations measured. This line symmetry at alkaline pH remains up to 50 °C as shown later for pH 11.8 in Figure 4.

At pH 12.1 and with increasing sodium oleate concentration, the center position of the line of the magnetic field shifts toward a lower magnetic field, and the line width increases; in both cases, a constant value is reached above 15 mM (data not shown). This indicates that the 16-DS molecules are distributed between the micelles and the bulk aqueous domain with a change of the equilibrium position toward micelles as the oleate concentration is increased. Above 15 mM oleate, all the probe molecules are incorporated into micelles. The shift of the peak position toward lower magnetic field with increasing oleate concentration and the increase in line width with an increase in the concentration of oleate reflect a lower micropolarity in the case of micelles than in the case of the aqueous domain. This is reasonable because the micelle interior is certainly less polar than water because of the presence of the alkyl chains.

In the case of pH 6.4, the $M = -1$ line is symmetric at 25 mM (see Figure 2) up to 50 °C (see later in Figure 4), but overlapped lines appear below 15 mM oleic acid/oleate (data not shown).

Because the ESR spectra of 16-DS in the presence of 25 mM oleic acid/oleate above pH 10.4 and below pH 6.5 are symmetric, the values of the rotational correlation time, τ_c, could be estimated according to eq 1,[38] from the widths and heights of the ESR spectral lines at $M = +1$ and $M = -1$.

$$\tau_c = A\,\Delta H_{(M=+1)}[(I_{(M=+1)}/I_{(M=-1)})^{1/2} - 1] \qquad (1)$$

Here, $I_{(M=-1)}$ is the peak-to-peak height for the high-field line. The value of A is assumed to be 6.6×10^{-10}.[38] The estimated τ_c values (and the corresponding microviscosities)[39] determined for 16-DS in the oleic acid/oleate system are 3.9×10^{-10} s (4 cP) at pH 10.4 and 6.1×10^{-10} s at pH 6.4 (6 cP); see Table 1.[40] Whereas τ_c of 16-DS in pure water is 9.3×10^{-11} s (1 cP), the τ_c values of 16-DS in octane and methanol are 5.34×10^{-11} s (0.5 cP) and 1.98×10^{-11} s (0.2 cP), respectively. Corresponding values for 16-DS in pure oleic acid, in SDS micelles, and in egg PC vesicles are also given (see Table 1 and Discussion).

Table 1. Rotational Correctional Time, τ_c, and Microviscosity of 16-DS

	τ_c/s	microviscosity/cP
25 mM oleic acid/oleate (pH 12.4−11)	$(3.8-3.9) \times 10^{-10}$	4
25 mM oleic acid/oleate (pH 7−6)	$(6.0-6.1) \times 10^{-10}$	6
water	9.3×10^{-11}	1
octane	5.3×10^{-11}	0.5
methanol	2.0×10^{-11}	0.2
pure oleic acid	1.0×10^{-9}	10.7
egg leicithin vesicle	9.1×10^{-10}	9.8
aq SDS soln (10%)	3.2×10^{-10}	3.4

(c) The Case at Intermediate pH (10.4 > pH > 6.4). The ESR line at $M = -1$ of 16-DS in the oleic acid/oleate system is asymmetric at intermediate pH, as a result of the overlapping of two lines. Measurements at pH 8.5 up to 50 mM oleic acid/oleate showed that the asymmetry of the $M = -1$ line remained within this entire concentration range, although the peak shape changes gradually with a change in the oleic acid/oleate concentration (spectra not shown).

The temperature dependence of the $M = -1$ line measured at pH 8.5 and pH 7.9 is shown in Figure 4, together with the spectra obtained at pH 11.8 and pH 6.3. As a general result, one can state that all qualitative observations made at 25 °C were confirmed between 10 and 50 °C; in particular, the ESR line at $M = -1$ is always asymmetric at the two intermediate pH values 8.5 and 7.9, whereas the $M = -1$ line at pH 11.8 and pH 6.3 remains symmetric.[41] The increased peak intensities at higher pH are due to an increase in the viscosity and correspondingly to an increase in τ_c, according to the Debye−Stokes−Einstein relation.

ESR Spectral Simulation. ESR spectral simulations were limited to the high-field line (at $M = -1$) because the shape of this line varied most notably among all three ESR lines. Details about the analysis are given in the Appendix.

As shown in Figure 5A−C, the simulation yielded a satisfactory separation of the experimental ESR line (the upper figures) into two lines (the lower figures). The total concentration of oleic acid + oleate was 25 mM, and the pH values were 9.4 (Figure 5A), 8.5 (Figure 5B), and 7.7 (Figure 5C), respectively, at a temperature of 20 °C. The resolved lines which were analyzed according to the modified Bloch equation correspond to the $M = -1$ line of the spin probe localized in two different types of

(38) Yoshioka, H. J. *J. Colloid Interface Sci.* **1978**, *63*, 378.

(39) Taking into account that τ_c generally depends on the microviscosity of the environment and that the microviscosity of water is nearly 1 cP, the corresponding microviscosities can be estimated, according to the following Debye−Stokes−Einstein equation: $\tau_c = (4\pi\eta a^3)/(3kT)$, where a is the average radius of the molecules and η is the viscosity of the medium; see: Yoshioka, H. *Chem. Lett.* **1977**, 1477−1478.

(40) Because of the overlapping ESR lines, an estimation of τ_c for the intermediate pH range was not possible.

(41) One general problem in using spin probes is the chemical difference between the relevant components of the system (oleic acid and oleate) and the actual spin probe applied. In the case of 16-DS and oleic acid, the melting points are for example 47−55 and 13−14 °C, respectively. For this reason, the investigation of the temperature dependency seemed to us to be of considerable importance.

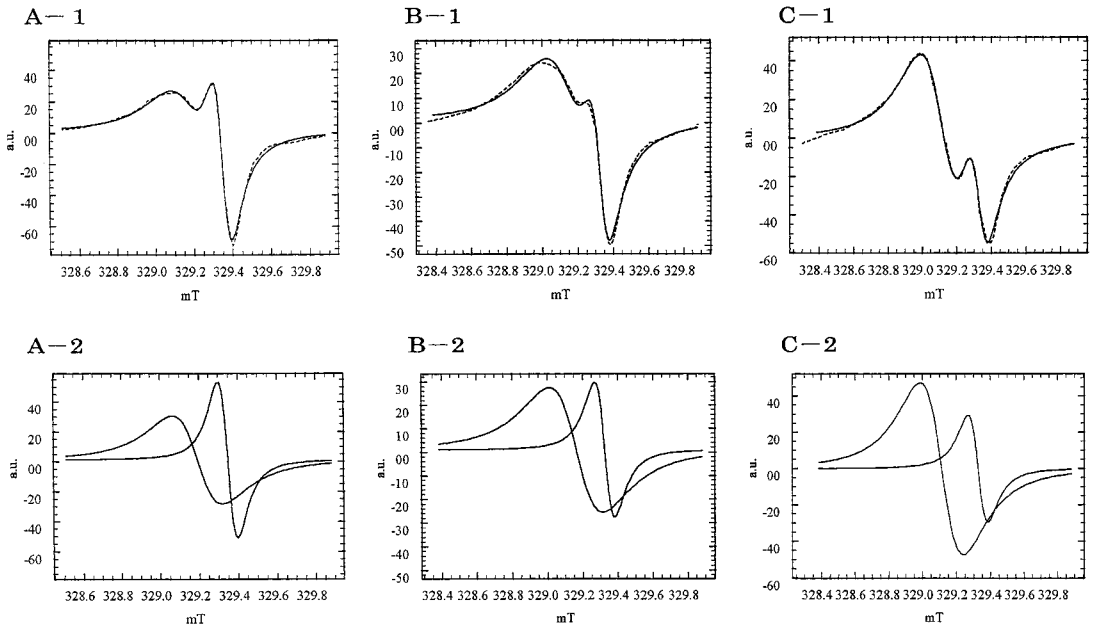

Figure 5. Separation of the ESR spectrum of 16-DS in an aqueous oleic acid/oleate system at pH 9.4 (A), pH 8.5 (B), and pH 7.7 (C) into two components. $T = 20$ °C. The concentration of oleic acid/oleate was 25 mM. (1, upper spectra): Dotted spectra in (A), (B), and (C) are experimental, and solid spectra are simulated. (2, lower spectra): The simulated spectra are separated into two components according to the modified Bloch equation (see Appendix).

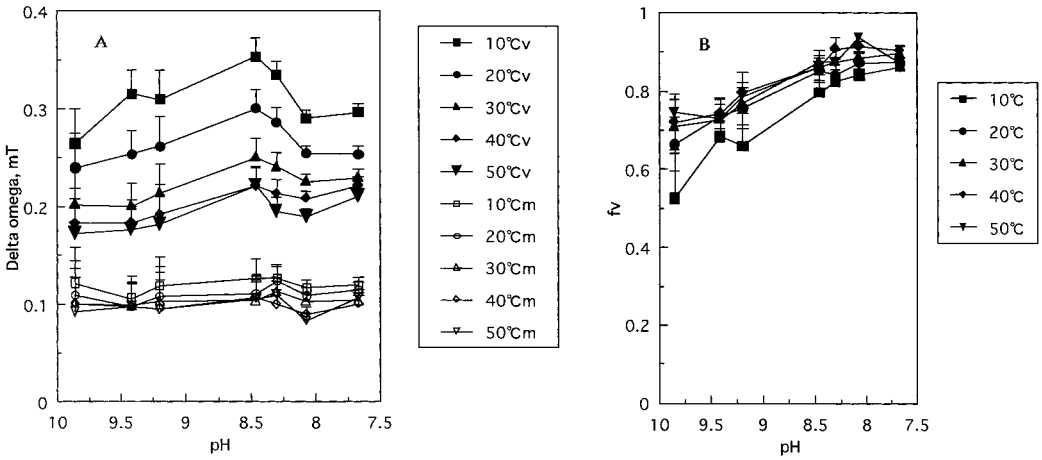

Figure 6. Dependency of the peak-to-peak width for 16-DS in the vesicles and micellar aggregates (A) and dependency of f_v, the fraction of 16-DS in the vesicles (B), against pH at 10−50 °C as obtained from ESR spectral simulation. The concentration of oleic acid + oleate was 25 mM. v, vesicular aggregates; m, micellar (nonlamellar) aggregates.

surfactant aggregates (see Appendix). The broader lines at the low magnetic field and the narrow lines at the high magnetic field (Figure 5, parts A-2, B-2, and C-2) are considered to be vesicles and nonlamellar aggregates (most likely nonspherical micelles), respectively; see Discussion.[42]

In the following, the oleic acid/oleate system is analyzed in more detail based on the ESR spectral simulation. The peak-to-peak widths for vesicular and micellar (nonlamellar) spin probe molecules ($\Delta\omega_v$, $\Delta\omega_m$) and f_v (the fractions of 16-DS in vesicles) as a function of pH and total oleic acid/oleate concentration are shown in Figures 6 and 7.

Figure 6A shows $\Delta\omega_v$ and $\Delta\omega_m$ as a function of pH between 10 and 50 °C, at a total concentration of oleic acid + oleate of 25 mM. (The value of $\Delta\omega_m$ actually corresponds to the mean width of 16-DS distributed between the micelles and the aqueous domain.) The highest value for $\Delta\omega_v$ is obtained at pH 8.5.

In Figure 6B, the fraction of the spin probe present in the vesicles, f_v, is plotted against pH.[43] As expected, the lower the pH, the higher the amount of vesicles (or more precisely bilayers).[44] Furthermore, f_v increases with temperature in the high pH region but remains almost constant at low pH.

Figure 7A shows the dependency of the line widths on the total concentration of oleic acid + oleate at 20 °C for 16-DS in the vesicles and in the micellar aggregates at pH 9.8 and 8.0. At both pH values, the peak-to-peak line width for the micelles ($\Delta\omega_m$) tends to increase with an increase in the total oleic acid + oleate concentration.

(42) Please note that in the case of micelles, the spin probe rapidly equilibrates between the micellar aggregates and the bulk aqueous domain of the system.

(43) Because in all the experiments analyzed in Figure 6B the total concentration of oleic acid + oleate was 25 mM, the concentration of the distributed probe molecules in the micellar aggregates was estimated to be between 3 and 5 mM within pH 9.9 and 7.7.

(44) Because we have no information about the size and lamellarity of the vesicles, we do not know whether the actual number of vesicles changes.

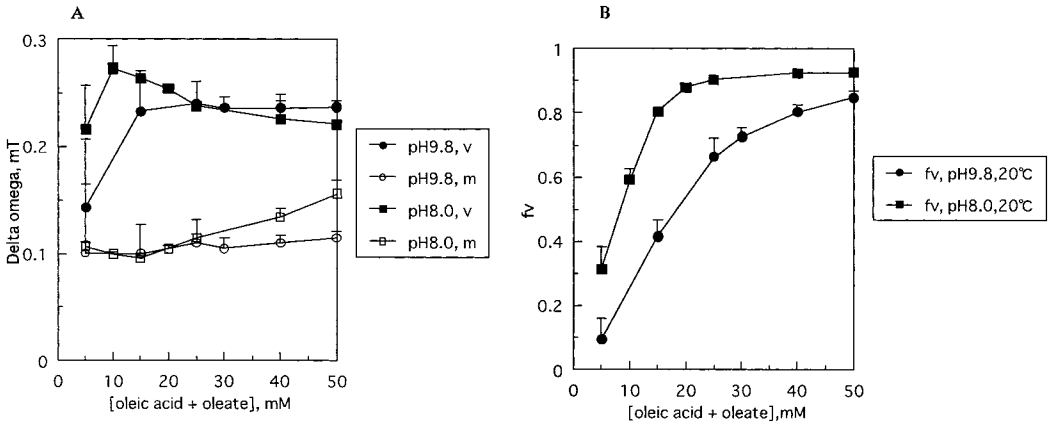

Figure 7. Dependency of the line widths for 16-DS in the vesicles and the micellar (nonlamellar) aggregates (A) and dependency of f_v, the fraction of 16-DS in the vesicles (B), against concentration of oleic acid + oleate at pH 9.8 and pH 8.0 as obtained from ESR spectral simulation. Temperature, 20 °C; v, vesicular aggregates; m, micellar (nonlamellar) aggregates.

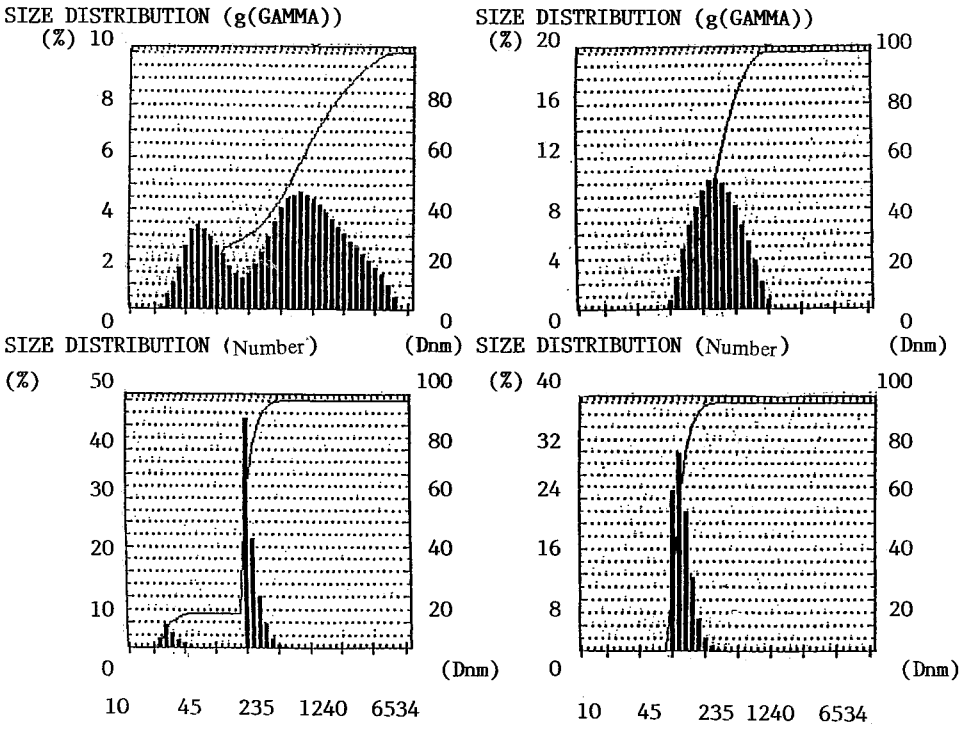

Figure 8. Histogram of 25 mM sodium oleate/oleic acid aggregates at pH 9.7 (refractive index, 1.3314; viscosity, 0.9021 cP) and pH 7.2 (refractive index, 1.3314; viscosity, 0.9018 cP), as obtained by electrophoretic light scattering at a scattering angle of 90° and a temperature of 24.4 °C.

Figure 7B shows that f_v increases with increasing concentration of oleic acid + oleate at pH 9.8 and pH 8.0 at 20 °C. This means that f_m decreases correspondingly ($f_v + f_m = 1$). The relative amount of spin probe molecules incorporated in vesicles at 5 mM is rather low in comparison with 50 mM oleic acid + oleate.

Electrophoretic Light Scattering Measurements. In an attempt to get information about the whole system from independent measurements, electrophoretic light scattering measurements were carried out. Figure 8 shows the size distributions obtained for the aggregates at pH 9.7 and pH 7.2 as measured by this technique. At pH 9.7, there are two kinds of aggregates with apparent mean diameters of 240 and 20 nm. However, only one type of aggregate (mean diameter ca. 100 nm) could be detected below pH 9.[45]

Discussion

Observations Made at High pH (pH > 10.4). From literature, it has been well-known for many years that oleate micelles are formed in the alkaline pH region. Small-angle X-ray scattering measurements indicated that the micelles are spherical at low concentration and become rodlike (or cylindrical) at higher concentration.[13,33] Recently, support for the presence of cylindrical micelles at pH 10.7 could be obtained from a cryo-transmission electron microscopy study.[27] Oleate micelles are expected to be in equilibrium with oleate monomers (and/or dimers[46]) at a concentration of possibly about 0.7−1.4 mM, the cmc value previously determined conductometrically[23] or colorimetrically.[24]

(45) The distribution of particle size(g(GAMMA)) and distribution of particle size(number) in Figure 8 mean distributions of scattering intensity of particles and of particle number, respectively. Because the number of particles depends on the scattering and the size of particles, some weight coefficient which is characteristic of ELS 800 is multiplied to convert the distribution of particle size(g(GAMMA)) into that of particle size(number). Then, the size distribution of the number shifts to a smaller size distribution.

(46) Somasundaran, P.; Ananthapadmanabhan, K. P.; Ivanov, I. B. *J. Colloid Interface Sci.* **1984**, *99*, 128−135.

The ESR measurements carried out in the present work indicate that the spin probe molecules (16-DS) in alkaline oleate solution appear to be present in a single environment in the entire oleate concentration range studied (up to 50 mM; see the spectral symmetry, shown in Figure 2). Because some of the probe molecules are expected to exist in the aqueous domain as monomers and some are expected to be incorporated into oleate micelles, the presence of a symmetric ESR line, at high as well as at low oleate concentration, indicates that the exchange of surfactant molecules between the aqueous domain and the micelles is faster than the time scale of the ESR measurements (10^{-10}–10^{-8} s). However, they seemed to be inconsistent with the currently accepted range of values. This is interpreted as follows. Because some of the probe molecules are expected to exist in the aqueous domain as monomers and some are expected to be incorporated into oleate micelles, the presence of only one symmetric ESR line, at high as well as at low oleate concentration, reflects that the transition rate from water to micelles is faster than the time scale of the ESR measurements (10^{-10}–10^{-8} s) and the line due to the probe in water shifted and coalesced with the line of the probe in the micelle.

Strictly, the transition rate from water to micelle (P_{wm}) is different from that from micelle to water (P_{mw}). If the concentrations of respective probes in micelles and water are C_m and C_w, the following equation is indicated.

$$C_m P_{mw} = C_w P_{wm}$$

In the case of the probe in the oleate micellar system, C_w is very low. As a result, P_{wm} must be large. In other words, this analysis means that the rate from water phase to micelles depends on cmc.

From Table 1, it can be seen that the microviscosity of oleate micelles (4 cP) is comparable to that of SDS micelles (3 cP).

Observations Made at Intermediate pH (10.4 > pH > 6.4). When the pH is lowered below 10.2, the solution becomes turbid (Figure 1), suggesting that a transition from the relatively small micelles to considerably larger aggregates, which scatter visible light, starts to occur. It has been reported before that at intermediate pH, the oleate/oleic acid system exists as bimolecular layers (bilayers).[5–9,11–13,25,47]

There has been also indisputable accumulation of data (especially electron and light microscopic observations)[1,2,8] showing that the bilayers are forming closed structures (spherical vesicles and tubular structures). However, the ESR measurements carried out in the present work indicate that the probe molecules (16-DS) incorporated into the oleic acid/oleate system are present in two different states within the entire intermediate pH range (see the high field line asymmetry in Figure 2). This particular peak at $M = -1$ was analyzed by separating it into two individual peaks by using a modified Bloch equation (see Appendix), as described above.

There are basically the following three possibilities for the two different environments: (i) two types of bilayers (e.g., vesicles of different sizes or vesicles and flat bilayer sheets); (ii) protonated and ionized probe molecules; (iii) two different types of aggregates (bilayers and nonlamellar aggregates). Out of these three possibilities, we exclude (i) and (ii) by the following control experiments.

First, a series of ESR measurements were carried by using extruded vesicle suspensions. The suspensions (25 mM oleic acid + oleate, pH 8.5) were passed several times through polycarbonate filters with mean pore diameters of 200 and 50 nm, to reduce the lamellarity of the vesicles and particularly their size to about 50 nm.[48] The corresponding ESR spectra, however, remained essentially unchanged compared with the suspension prepared without extrusion. This indicates that the vesicle size (the bilayer curvature) has no significant influence on the 16-DS ESR signal, which excludes the possibility in (i).

Second, in contrast to 5-DS (5-doxylstearic acid),[49] the line shape of the ESR spectrum of 16-DS incorporated into egg phosphatidylcholine vesicles measured at pH 12.3, pH 8.8, and pH 6.8 is independent of pH (data not shown),[50] excluding the possibility in (ii). Furthermore, the ESR spectrum of 16-DS solubilized in micelles of SDS or *n*-octyl glucoside is always symmetric.[51] On the basis of these observations, we postulate that nonlamellar aggregates (possibility nonspherical micelles) coexist with bilayers (vesicles). Electrophoretic light scattering measurements indeed confirm the presence of two types of aggregates of different sizes, at least at the high end of the intermediate pH range (pH 9.7), whereas the second type of aggregate could not be detected at lower pH (below pH 9.0). This observation is consistent with the ESR spectral simulation as a function of pH, which indicates that the amount of nonlamellar (micellar) aggregates decreases with decreasing pH.

The coexistence of vesicles and nonlamellar aggregates was also supported by the results in Figure 3, where the peak height, the peak width, and a_N shifted continuously with decreasing pH.

Interestingly, the line width corresponding to the vesicles ($\Delta\omega_v$) showed a maximal value at pH 8.5 (highest rigidity); see Figure 6A. This pH value is essentially the pH at which (in earlier experiments) giant oleic acid/oleate vesicles formed most easily upon dilution of a more concentrated system.[26] This pH value coincides with the apparent pK_a of oleic acid in the system.[21] Furthermore, earlier surface tension measurements of oleic acid monolayers at the water–air interface as a function of pH of the aqueous subphase have shown that the interfacial tension assumes a minimum value at pH 8.5,[52] at conditions where the monolayer has the highest stability.

The titration curve (Figure 1) and observations by eye indicated that large, condensed aggregates occurred below pH 8.0. The structure of these aggregates remains largely unclear. From the ESR spectra, we could not distinguish them from bilayers. Therefore, the nature of the coexisting aggregation forms remains open within the pH range between 6.4 and 8.0, although the ESR spectra clearly indicated the presence of two different states of 16-DS.

Observations Made at Low pH (pH < 6.4). The ESR measurements in the low pH region indicate that the 16-DS probe molecules exist in a single environment, as long as the oleic acid/oleate concentration are sufficiently high.

(47) In the pH region at which the pH equals approximately the pK_a of oleic acid in the bilayer (pH 8–9), an approximately equimolar mixture of the protonated and the ionized form of the acid allows the formation of cylindrical dimer structures in which the hydrophobic tails lie parallel and a hydrogen bond may form between the carboxylic acid and the carboxylate headgroup. This hydrogen bonding eliminates the electrostatic headgroup repulsions present in the micelles and favors the formation of bilayers, which are less curved than micelles.

(48) Mayer, L. D.; Hope, M. J.; Cullis, P. R. *Biochim. Biophys. Acta* **1986**, *858*, 161–168.

(49) Sanson, A.; Ptak, M.; Rigaud, J. L.; Gary-Bobo, C. M. *Chem. Phys. Lipids* **1976**, *17*, 435–444.

(50) The pK_a of stearic acid in phosphatidylcholine vesicles has been determined to be around 7.3 (37 °C): Ptak, M.; Egret-Charlier, M.; Sanson, A.; Bouloussa, O. *Biochim. Biophys. Acta* **1980**, *600*, 387–397.

(51) Yoshioka, H. *J. Colloid Interface Sci.* **1978**, *66*, 352–354.

(52) Somasundaran, P.; Ananthapadmanabhan, K. P. In *Solution Chemistry of Surfactants*; Mittal, K. L., Ed.; Plenum Press: New York, 1979; Vol. 2, pp 777–800.

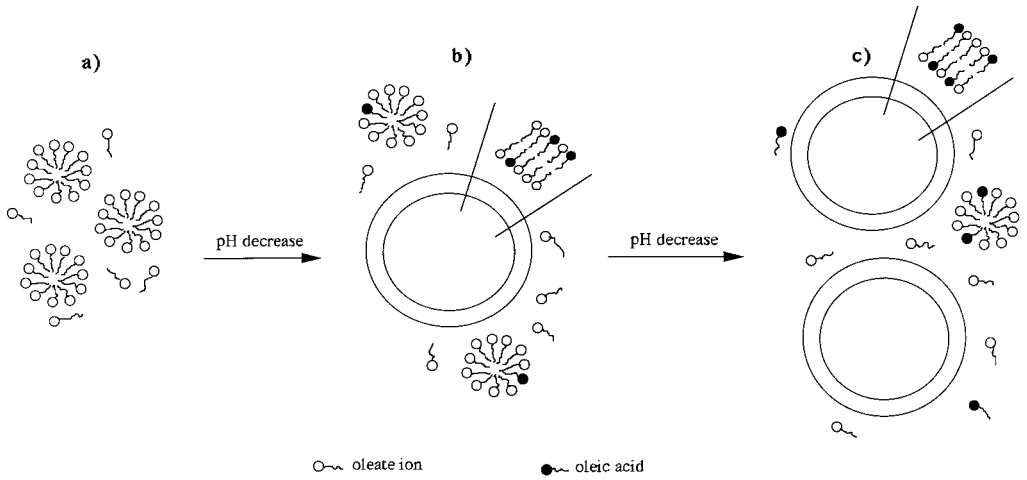

Figure 9. Schematic representation of the transformation of micelles to vesicles upon lowering the pH of an alkaline oleate solution above the cmc for oleate. The presence of nonvesicular aggregates at intermediate pH is one of the results obtained in the present ESR study.

At low concentrations, we observed a splitting of the high-field line at $M = -1$, indicating that the probe molecules exist in two different states. The microviscosity (6 cP) is considerably lower than in the case of neat oleic acid (11 cP). Therefore, the aggregates must be in a different state from the neat oleic acid oil. It is possible that this state consists of condensed, relatively dry lamellar bilayers which may be separated from the aqueous phase by a surface layer of oleic acid molecules. These structures tend to aggregate and separate from the aqueous solution; they are not as rigid as hydrated egg PC bilayers.

Concluding Remarks

On the basis of the results presented and discussed above, a summary of the transformation of oleate micelles upon lowering the pH is presented in the schematic drawing in Figure 9. Above pH 10.4, oleate micelles exist in equilibrium with monomers. The concentration of the oleate monomers is close to the cmc of ~1 mM (Figure 9a). The spin probe exchanges quickly the position between the micelles and the aqueous domain. With decreasing pH, oleate gets more and more protonated and the protonated form, oleic acid, is expected to interact with the oleate ion, bringing about the formation of bilayers (vesicles); micelles are still present (Figure 9b). The ESR data indicate that bilayers, nonlamellar aggregates (most likely micelles), and monomers always coexist in the intermediate pH range ($8.0 < \text{pH} < 10.4$).[53] The 16-DS spin probe molecules are distributed between vesicles, micelles, and the aqueous phase. Whereas 16-DS can exchange quickly the position between the micelles and the aqueous domain, it exchanges only slowly between the bilayers (vesicles). The ESR spectral simulation allowed determination of the relative amounts of micellized 16-DS and vesicularized 16-DS. Within the region of pH 10−8.5, the fraction of surfactants in the vesicle (f_v) increases gradually with decrease of pH, indicating that the transformation of the micelles to the vesicles occurs continuously with decrease of pH.

The dilution induced the increase of the micellar aggregates (Figure 7). This phenomenon was assumed as follows. It is well-known that dilution of a micellar solution results in an increase of the ratio of monomer as well as a decrease of the ratio of micelle and further the dilution of lamellar type aggregates which are formed at a high concentration of surfactant leads to the formation of micelles. Because the size of micelles is fairly small compared to that of vesicles and the extent of molecular interaction in the vesicle is higher than that in micelles in the equilibrium system of vesicles/micelles, it is assumed that vesicles may be enthalpically stable, but micelles may be entropically stable in the overall system. In a high concentration of oleic acid/oleate, as the molecules make an approach to each other and they interact mutually, the vesicles exist favorably. On the other hand, in the diluted solution the number of micelles which are entropically stable comes to increase to compensate the enthalpic instability of the micelle. Therefore, it is considered that the dilution of a mixture solution of micelles/vesicles results in an increase of the ratio of micelles as well as a decrease of the ratio of vesicles. This is one of the dynamic properties of the oleic acid/oleate system.

In conclusion, the oleic acid/oleate system in the intermediate pH region is a dynamic system that is significantly different from a conventional phospholipid system. Further independent studies will be necessary to support the general findings of the present study and to shed light on the structure of the nonlamellar (micellar) aggregates proposed to coexist with vesicles in the intermediate pH range.

Acknowledgment. We are grateful to Mr. Ayumi Kasahara, Miss Yumi Imaseki, and Miss Shiho Sato of the University of Shizuoka for technical assistance.

Appendix

In the case where spin probe molecules exchange their positions between two different sites within the system relatively slowly, the application of a modified Bloch equation is one of the most useful techniques to simulate the line shape of such a chemical exchange system. Yoshioka and Kazama[54] already applied this equation successfully to simulate the ESR spectrum of a spin probe distributed between the polar sites of the water pools and the nonpolar sites of the bulk solution in a reversed

(53) In a first approximation, the concentration of the monomer, which coexists with the micelles, is assumed to correspond approximately to the cmc. The effective monomer concentration is expected to decrease with decreasing pH[22] because the solubility of oleic acid is much lower than that of the oleate salt.

(54) Yoshioka, H.; Kazama, S. *J. Colloid Interface Sci.* **1983**, *95*, 240−246.

micellar system. The solution of the modified Bloch equation is[55]

$$F(\omega) = f_v(\omega - \hat{\omega}_m) + f_m(\omega - \hat{\omega}_v) + j(P_{vm} + P_{mv})/ [(\omega - \hat{\omega}_v) + jP_{vm}][(\omega - \hat{\omega}_m) + jP_{mv}] + P_{vm}P_{mv}$$

Here, the ESR spectrum is a function of the angular frequency, ω; f_v and f_m are the fractions of the probe (16-DS) located in the vesicles (v) and in the micelles (m), respectively; j is the imaginary part; $\hat{\omega}_v$ and $\hat{\omega}_m$ are correlated with the positions of the original lines ω_v and ω_m and the spin−spin relaxation time (T_2).

$$\hat{\omega}_m = \omega_m - j/T_{2m}$$

$$\hat{\omega}_v = \omega_v - j/T_{2v}$$

T_2 is related to the peak-to-peak width ($\Delta\omega$) of the original lines of the doublet assuming that the line shape is Lorentzian.[56]

$$\Delta\omega_m = 2/\sqrt{3}T_{2m}$$

$$\Delta\omega_v = 2/\sqrt{3}T_{2v}$$

P_{vm} and P_{mv} are the probabilities of 16-DS transferring from the vesicles to the micelles and from the micelles to the vesicles, respectively. P_{vm} and P_{mv} are almost zero, as discussed in the bulk text. Because the original lines are always Lorentzian, the integrated intensity of the absorption line is proportional to the product of the peak-to-peak height and the square of the width, as follows.

$$f_v{:}f_m = h_v(\Delta\omega_v)^2{:}h_m(\Delta\omega_m)^2$$

where h_v and h_m are the peak-to-peak heights of the lines. Although theoretical treatments of ESR spectra are generally carried out as a function of the angular frequency (ω), it is possible to change the function into a dependency on the magnetic field **H**.[54]

The imaginary part of the function $F(\omega)$ given above yields the line shape of the absorption spectrum. The ESR spectrum, however, was recorded as the first derivative of the absorption line. Therefore, the imaginary part was differentiated with ω and was calculated by using six parameters, $\Delta\omega_m$, $\Delta\omega_v$, ω_m, ω_v, f_v, and f_m ($= 1 - f_v$). In this case, the parameters were obtained by the revised Marquardt method using $n > 100$ observation points, ω_i, $i = 1,2,...,n$, of the ESR spectrum, and their asymptotic 95% confidence intervals were estimated according to a nonlinear regression analysis. For $M = 5$ parameters (θ_1, θ_2, θ_3, θ_4, θ_5) = ($\Delta\omega_m$, $\Delta\omega_v$, ω_m, ω_v, f_v), the asymptotic 95% confidence interval for θ_1 is given by

$$t_{n-m}^{2.5\%}\sqrt{\frac{S}{n-m}(A^{-1})_i}$$

where S is the error sum of squares, $t_{n-m}^{2.5\%}$ is the upper 2.5% percentage point of the t-distribution with $n - M$ degrees of freedom, and the $M \times M$ matrix

$$(A)_{ij} = \sum_{k=1}^{n} \mathrm{Im}\left[\frac{\partial^2 F(\omega_k)}{\partial\omega_k\partial\theta_i}\right] \mathrm{Im}\left[\frac{\partial^2 F(\bar{\omega}_k)}{\partial\omega_k\partial\theta_j}\right]$$

The asymptotic confidence intervals can be regarded as the true confidence interval because of the large number of observation points. Thus, we regard them simply as the errors of the estimated parameters.

LA0100338

(55) Carington, A.; MacLachlan, A. D. *Introduction to Magnetic Resonance*; Harper and Low: New York, 1967.

(56) Quite generally, the good agreement between the experimental ESR spectra and the simulated lines shown in Figure 6 indicates that the assumption of a Lorentzian line shape is reasonable and did not cause serious errors.